TTI-237: A Novel Microtubule-Active Compound with *In vivo* Antitumor Activity

Carl F. Beyer,[1] Nan Zhang,[2] Richard Hernandez,[1] Danielle Vitale,[1] Judy Lucas,[1] Thai Nguyen,[2] Carolyn Discafani,[1] Semiramis Ayral-Kaloustian,[2] and James J. Gibbons[1]

[1]Discovery Oncology and [2]Medicinal Chemistry, Chemical and Screening Sciences, Wyeth Research, Pearl River, New York

Abstract

5-Chloro-6-[2,6-difluoro-4-[3-(methylamino)propoxy]phenyl]-*N*-[(1*S*)-2,2,2-trifluoro-1-methylethyl]-[1,2,4]triazolo[1,5-*a*]pyrimidin-7-amine butanedioate (TTI-237) is a microtubule-active compound of novel structure and function. Structurally, it is one of a class of compounds, triazolo[1,5a]-pyrimidines, previously not known to bind to tubulin. Functionally, TTI-237 inhibited the binding of [^{3}H]vinblastine to tubulin, but it caused a marked increase in turbidity development that more closely resembled the effect observed with docetaxel than that observed with vincristine. The morphologic character of the presumptive polymer is unknown at present. When applied to cultured human tumor cells at concentrations near its IC_{50} value for cytotoxicity (34 nmol/L), TTI-237 induced multiple spindle poles and multinuclear cells, as did paclitaxel, but not vincristine or colchicine. Flow cytometry experiments revealed that, at low concentrations (20–40 nmol/L), TTI-237 produced sub-G_1 nuclei and, at concentrations above 50 nmol/L, it caused a strong G_2-M block. The compound was a weak substrate of multidrug resistance 1 (multidrug resistance transporter or P-glycoprotein). In a cell line expressing a high level of P-glycoprotein, the IC_{50} of TTI-237 increased 25-fold whereas those of paclitaxel and vincristine increased 806-fold and 925-fold, respectively. TTI-237 was not recognized by the MRP or MXR transporters. TTI-237 was active *in vivo* in several nude mouse xenograft models of human cancer, including LoVo human colon carcinoma and U87-MG human glioblastoma, when dosed i.v. or p.o. Thus, TTI-237 has a set of properties that distinguish it from other classes of microtubule-active compounds. [Cancer Res 2008;68(7):2292–300]

Introduction

Microtubules, composed mainly of αβ-tubulin heterodimers and also numerous associated proteins, are macromolecular structures that participate in many crucial cellular functions (1). Microtubules are a proven target in cancer treatment because they are part of the mitotic spindle, the complex and dynamic structure that mediates chromosome separation at mitosis (2–5). Without a functional spindle, cells cannot divide correctly and typically undergo apoptosis (6). The discovery of new antimitotic compounds, both those targeting microtubules and those targeting other components of the mitotic machinery, has received much attention (7, 8).

At the present time, there are two categories of tubulin-binding compounds that are approved for cancer therapy: *Vinca* alkaloids (vincristine, vinblastine, vinorelbine, and vindesine) and taxanes (paclitaxel and docetaxel). *Vinca* alkaloids bind at one of three known pharmacologic sites on the tubulin heterodimer, called the *Vinca* site (3). Many other compounds, mostly natural products, also bind at or near this site (9, 10); collectively, the region of the protein where these compounds bind is called the *Vinca* domain. *Vinca* domain ligands destabilize microtubules and inhibit microtubule formation. Taxanes (and several other classes of natural products; ref. 11) bind at the taxane site to stabilize and promote formation of microtubules, the opposite effects of *Vincas*. A third site, defined by colchicine, also binds many ligands, both natural and synthetic, all of which destabilize microtubules and inhibit their formation. We report here a new compound, 5-chloro-6-[2,6-difluoro-4-[3-(methylamino)propoxy]phenyl]-*N*-[(1*S*)-2,2,2-trifluoro-1-methylethyl]-[1,2,4]triazolo[1,5-*a*]pyrimidin-7-amine butanedioate (TTI-237; Fig. 1), that differs in significant ways from known tubulin ligands. TTI-237 may be the prototype of a new category of tubulin-binding compound. It is potent and shows *in vivo* antitumor activity in xenograft models.

Materials and Methods

Materials

TTI-237, as the free base, the hydrochloride salt, or the succinate salt, was synthesized as described (12). In all cases, the compound was used as a stock solution in DMSO and was stored at −20°C. Paclitaxel, vincristine, and colchicine were obtained from Sigma, and docetaxel was obtained from LKT Laboratories, Inc.; all were used as stock solutions in DMSO with storage at −20°C. Microtubule-associated protein (MAP)-rich tubulin, also called microtubule protein, containing ~70% tubulin and 30% MAPs (ML113), and highly purified tubulin (>99% pure; TL238), both from bovine brain, were obtained from Cytoskeleton, Inc. Both of these were lyophilized products and contained small amounts of guanosine 5′-triphosphate (GTP; approximately equivalent to 0.5 mmol/L GTP when the protein concentration was 10 mg/mL). PEM buffer [80 mmol/L piperazine-*N*,*N*′-*bis*[2-ethanesulfonic acid] (pH 6.9), 1 mmol/L ethylene glycol-*bis*(β-aminoethyl ether)-*N*,*N*,*N*′,*N*′-tetraacetic acid, 1 mmol/L magnesium chloride], GTP, and the advanced protein assay reagent were also obtained from Cytoskeleton. Glycerol was purchased from Pierce, and 2′,3′-dideoxy-GTP was from Sigma.

[^{3}H]Vinblastine (specific activity, 9.6 Ci/mmol) and MicroSpin G-50 columns were obtained from Amersham Biosciences; columns were prepared for use according to the manufacturer's instructions. [^{3}H]Colchicine (specific activity, 76.5 Ci/mmol) was obtained from New England Nuclear, and [^{3}H]paclitaxel (specific activity, 14.7 Ci/mmol) was from Moravek Biochemicals.

Methods

Cell lines. Human cancer cell lines were obtained from the American Type Culture Collection, except for KB-3-1 (herein called KB, cloned from a human epidermoid carcinoma) and the derived lines KB-8-5 and KB-V1, which express moderate and very high levels of the multidrug resistance 1

Note: Supplementary data for this article are available at Cancer Research Online (http://cancerres.aacrjournals.org/).

Requests for reprints: Carl F. Beyer or Nan Zhang, Wyeth Research, 401 N. Middletown Road, Pearl River, NY 10965. Phone: 845-602-4421; E-mail: beyerc@wyeth.com or zhangn@wyeth.com.

doi:10.1158/0008-5472.CAN-07-1420

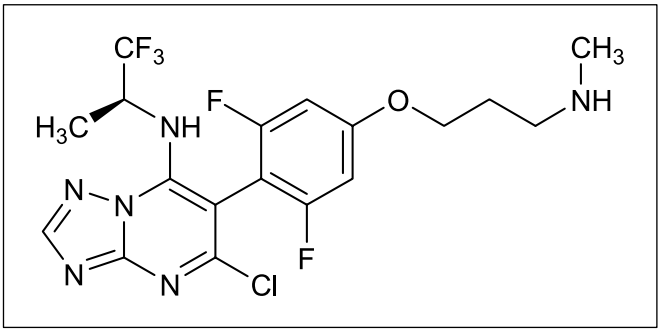

Figure 1. The structure of the free base of TTI-237.

(MDR1; P-glycoprotein) drug transporter protein, respectively, which were provided by Dr. M. Gottesman (National Cancer Institute; ref. 13) via Dr. L. Greenberger (Wyeth Research). Unless otherwise noted, all cell lines were cultured in RPMI 1640 with L-glutamine and supplemented with 10% heat-inactivated FCS, 100 units/mL penicillin, and 100 μg/mL streptomycin (all from Life Technologies). Cells were incubated at 37°C in humidified 5% CO_2 in air. Resistant cells were cultured without selective drug for at least 1 wk before use.

Cytotoxicity assay. Cells were harvested by trypsinization, washed, counted, and distributed to wells of 96-well flat-bottomed microtiter plates at 1,000 cells per well in 200 μL of medium. All plates were incubated at 37°C in humidified 5% CO_2 in air for ~24 h.

On day 2, compounds for test were diluted and added to wells. Compounds were dissolved in DMSO at 10 to 20 mmol/L. For each compound, nine serial 2-fold dilutions were prepared in DMSO. Ten microliters of each dilution was transferred to 100 μL of medium and mixed well, and then 5 μL of this dilution were transferred in triplicate or quadruplicate to wells containing cells. The final high concentration of each compound was typically 5 μmol/L. All cultures, including controls with no compound, contained a final concentration of 0.27% DMSO. After 3 d of culture with test compounds (day 5 overall), the MTS assay (Promega; CellTiter 96 aqueous nonradioactive cell proliferation assay) was done on all wells. The averaged replicates for each compound at each concentration level were plotted against concentration, and the concentration that produced a relative color yield half way between the maximum (no compound) and minimum (all cells killed) was taken as the IC_{50} value.

Tubulin polymerization experiments. Immediately before use, microtubule protein or purified tubulin was dissolved in ice-cold PEM buffer. When used, GTP was present in PEM buffer at 1 mmol/L. In the case of purified tubulin without added GTP, the PEM buffer contained 10% (w/v) glycerol. The tubulin solution was centrifuged at top speed in an Eppendorf model 5415C microcentrifuge (Brinkmann Instruments) for 10 min at 4°C to remove any particles or aggregates. The supernatant from this centrifugation was dispensed at 100 μL per well to wells of a half-area 96-well plate (Corning, Inc.) already containing 10 μL of the compounds of interest. Compounds were diluted in the same buffer used for tubulin solubilization before being added to wells. The final compound concentrations and tubulin concentration are given in figure legends. Each compound was tested in duplicate at each concentration in each experiment. The polymerization plate was prepared at room temperture, and the cold tubulin solution was the final addition. As rapidly as possible after tubulin addition, the plate was put in a SpectraMax Plus plate reader (Molecular Devices Corp.), thermostated at either 24°C or 35°C, and mixed for 15 s using the instrument mix function, and the absorbance of each well at 340 nm was determined every minute for 60 min. An increase in apparent absorbance at 340 nm over the course of the reaction was a measure of the appearance of turbidity believed to be caused by the formation of tubulin polymers of unknown morphology. The absorbance at time 0 for each well was subtracted from each of the subsequent absorbance readings for that well, and then the duplicates were averaged. Every other point is shown in Fig. 2 and Supplementary Figs. S1 to S3 for clarity.

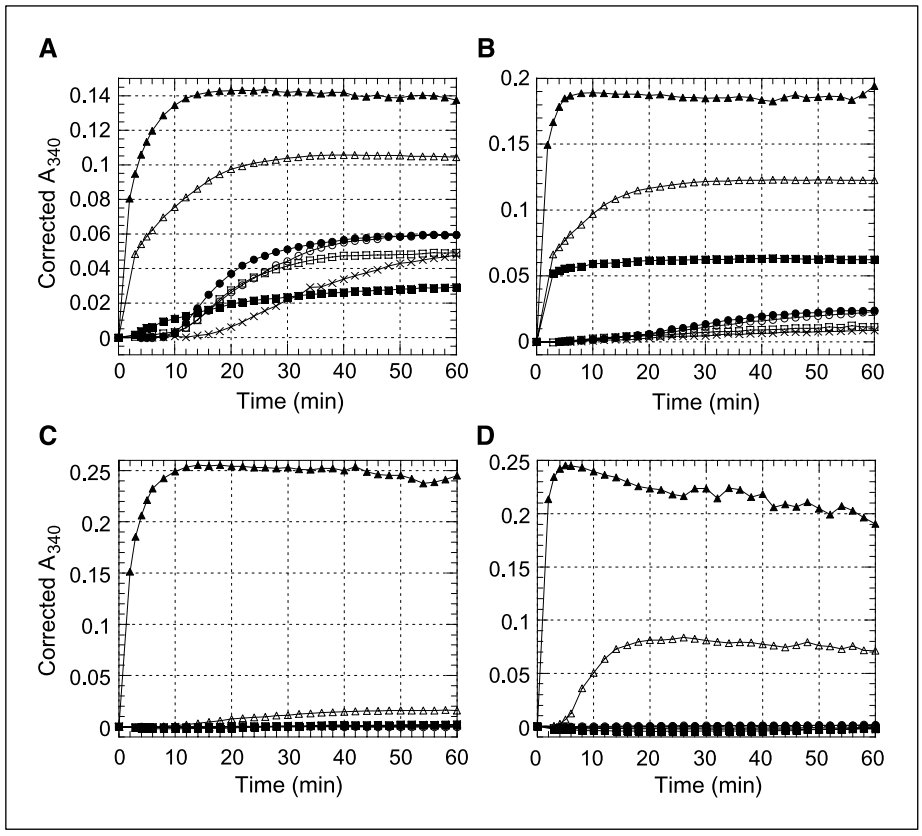

Figure 2. Effects of TTI-237 on tubulin polymerization. Effects of TTI-237 on the *in vitro* polymerization of microtubule protein plus 1 mmol/L GTP (*A*), microtubule protein without added GTP (*B*), highly purified tubulin plus 1 mmol/L GTP (*C*), highly purified tubulin without added GTP (*D*). Microtubule protein concentration (based on tubulin heterodimer) was ~10 μmol/L, and reaction temperature was 24°C in *A* and *B*. Purified tubulin concentration and temperature was 22.5 μmol/L and 24°C in *C* and 14.9 μmol/L and 35°C in *D*. The reactions in *D* also contained glycerol at 10% (w/v). Concentrations of TTI-237: ×, control (DMSO at the highest concentration used for experimental curves); ○, 0.1 μmol/L; ●, 0.3 μmol/L; □, 0.9 μmol/L; ■, 2.7 μmol/L; △, 8.1 μmol/L; ▲, 24.3 μmol/L. DMSO concentrations ranged from 0.002% to 0.485%.

To measure very rapid turbidity development that might occur before the first absorbance reading could be made, the background absorbance of each well of the empty reaction plate was taken before each assay. (Control experiments showed that the absorbance of the empty wells was the same as that of wells filled with unpolymerized tubulin starting solution.) If the time 0 absorbance reading differed from the background absorbance reading of that well, then the time 0 value was corrected accordingly.

Competitive binding experiments. To study possible competition at the *Vinca* domain and colchicine site, incubations were done under conditions which do not favor polymerization because vinblastine and colchicine bind preferentially to unpolymerized heterodimer. Highly purified tubulin was dissolved in PEM buffer without GTP and used at a final concentration of 1.0 to 1.3 mg/mL (10–13 μmol/L). Aliquots of competitor stock solutions were added to aliquots of the tubulin solution to give final concentrations of 100 μmol/L, and then aliquots of either [^{3}H]vinblastine or [^{3}H]colchicine were added to give final concentrations of 100 nmol/L or 50 nmol/L, respectively. Each reaction was run in quadruplicate. These solutions were incubated at 24°C for 1 h and then applied to MicroSpin G-50 columns which were centrifuged for 2 min at 3,000 rpm in an Eppendorf 5415C microfuge. An aliquot of each column effluent (containing tubulin and bound radioligand) was mixed with scintillation fluid and counted in a liquid scintillation spectrometer. Controls included samples without competitor and samples with unlabeled vincristine, colchicine, or paclitaxel. The ability of the competitor to inhibit the binding of the radioligand was expressed as a percentage of control binding in the absence of any competitor.

For competition with [^{3}H]paclitaxel, preformed microtubules were used because paclitaxel binds preferentially to microtubules rather than free heterodimer. Highly purified tubulin was dissolved in PEM buffer containing 0.75 mol/L glutamate and 25 μmol/L dideoxy-GTP; final protein concentration was 0.25 to 0.35 mg/mL (2.5–3.5 μmol/L). These conditions foster the rapid formation of short stable microtubule polymers (14). This solution was incubated for 30 min at 37°C to allow microtubules to form. Then aliquots of the microtubule solution were added to microfuge tubes already containing both [^{3}H]paclitaxel (final concentration of 2.1 μmol/L, 1.2 Ci/mmol) and competitors at the final concentrations given in the figures, and incubation at 37°C was continued for another 30 min. The samples were then centrifuged at top speed in an Eppendorf 5415C microfuge for 20 min at room temperature to pellet the microtubule protein. Triplicate aliquots of each supernatant were mixed with scintillation fluid and counted in a liquid scintillation spectrometer. From the amount of radioactivity in the supernatants and the measured total starting radioactivity, the amount of [^{3}H]paclitaxel bound to pelleted microtubule protein was calculated. In addition, duplicate aliquots of each supernatant were taken for analysis of protein content using the advanced protein assay. From the amount of protein in the supernatants and the measured total starting protein concentration, the amount of protein in the pellets was calculated. Controls included samples without competitor and samples with unlabeled vincristine, colchicine, or paclitaxel. The ability of each competitor to inhibit radioligand binding to pelleted protein and to change the amount of protein in the pellets was expressed as a percentage of control without any competitor.

Immunofluorescence microscopy. HeLa cells were cultured in DMEM containing 10% heat-inactivated fetal bovine serum, 100 units/mL penicillin, and 100 μg/mL streptomycin (all from Life Technologies). For experiments, cells were plated at 2.5×10^4 per 0.5 mL per chamber of Biocoat poly-D-lysine–coated eight-well culture slides (Becton Dickinson Labware). Compounds were added to chambers the next day in a volume of 5 μL DMSO, giving a final DMSO concentration of 1%. Twenty hours later, medium was removed from the wells, the chamber sides were lifted off, and cells were fixed with ice-cold methanol for a minimum of 10 min. The slides were removed from methanol and allowed to air-dry. All remaining steps were done at room temperature. The cells were washed with two changes of PBS (10 min each time, in a Copland jar), then incubated with anti α-tubulin monoclonal antibody (1:500 dilution, clone DM1-A, Sigma) in 1% bovine serum albumin (BSA; IgG free and protease free, from Jackson ImmunoResearch Laboratories) in PBS for 1 h. Cells were washed twice with PBS for 10 min each time, then incubated with secondary antibody [1:100 dilution of FITC-conjugated goat antimouse IgG, $F(ab')_2$ specific, Jackson ImmunoResearch] in 1% BSA in PBS for 1 h in the dark. After two washes with PBS, 5 min each, cells were stained with Hoechst 33258 (Molecular Probes) at 6 μg/mL in PBS for 10 min, followed by two PBS washes. Finally, cells were mounted in SlowFade Light (Molecular Probes) and examined with an Olympus BX61 microscope using a 40× UPlanApo air objective. Images were acquired with a Cooke SensiCam CCD imaging camera and Sliderule software.

Flow cytometry. HeLa cells were plated at 1.25×10^5 in 2 mL/well in 12-well plates and cultured overnight. Then various concentrations of compounds were added as indicated in the figures, and culture was continued for 18 h. Cells were then harvested, taking care to recover all nonadherent as well as adherent cells from each well. The recovered cells were processed using the Cycle Test Plus DNA reagent kit from Becton Dickinson. This kit contains reagents to dissolve cell membrane lipids with a nonionic detergent, degrade structural proteins with trypsin, remove RNA with RNase, and stabilize the nuclear chromatin with spermine. The cleaned, isolated nuclei were stained with propidium iodide and analyzed by flow cytometry using a FACSCalibur instrument from Becton Dickinson. Nuclei were analyzed instead of cells because this approach gives greater accuracy in DNA content estimates (15) and because we wished to detect nuclei from multinuclear cells, although mitotic cells, which lack a nuclear envelope, may not be accurately measured. Each compound was analyzed in three independent experiments, and data were averaged to make the graphs presented here. Estimates of the fraction of total nuclei in each cell cycle compartment were done by visually setting markers on the population histograms as illustrated in Fig. 5*B*.

Tumor xenograft experiments. Athymic nu/nu female mice were implanted s.c. in the flank with either 1×10^7 LoVo human colon adenocarcinoma cells or 1×10^6 U87-MG human glioblastoma cells. Cells were suspended in culture medium for injection. When tumors attained a mass of between 80 and 120 mg (day 0), animals were randomized into treatment groups each containing 5 to 10 animals. After staging, animals were treated i.v. or p.o. with TTI-237 formulated in 0.9% saline or Klucel according to the schedules given in the figure legend or with vehicle alone. Tumor volumes [(length × width^2) / 2] were determined at regular intervals. Results are reported as relative tumor growth (mean tumor volume on day measured divided by the mean tumor volume on day 0) as a function of time after staging. The data were analyzed by a one-sided Student's t test. A P value of ≤ 0.05 indicated a statistically significant reduction in tumor growth of the treated group compared with that of the vehicle control group.

Results

TTI-237 causes marked turbidity development with both microtubule protein and purified tubulin. Figure 2 shows the effects of TTI-237 on the aggregation of microtubule protein or pure tubulin in the presence or absence of 1 mmol/L GTP. TTI-237 was studied at six concentrations, ranging from below to above the concentration of tubulin. At 0.1, 0.3, and 0.9 μmol/L with microtubule protein (i.e., with tubulin in excess by a factor of ~100 to 11-fold), TTI-237 reduced the lag phase and enhanced the rate of aggregation compared with the control reaction without added compound (Fig. 2*A*). By comparison, docetaxel at the same concentrations had similar but quantitatively greater enhancing effects (Supplementary Fig. S1*A*), whereas vincristine progressively inhibited polymerization, such that at 0.9 μmol/L (and also at 2.7 μmol/L), microtubule formation was completely inhibited (Supplementary Fig. S2*A*). Colchicine also inhibited polymerization of microtubule protein in a dose-dependent manner (Supplementary Fig. S3*A*).

There was a qualitative change in the effect of TTI-237 on microtubule protein aggregation at a concentration of 2.7 μmol/L

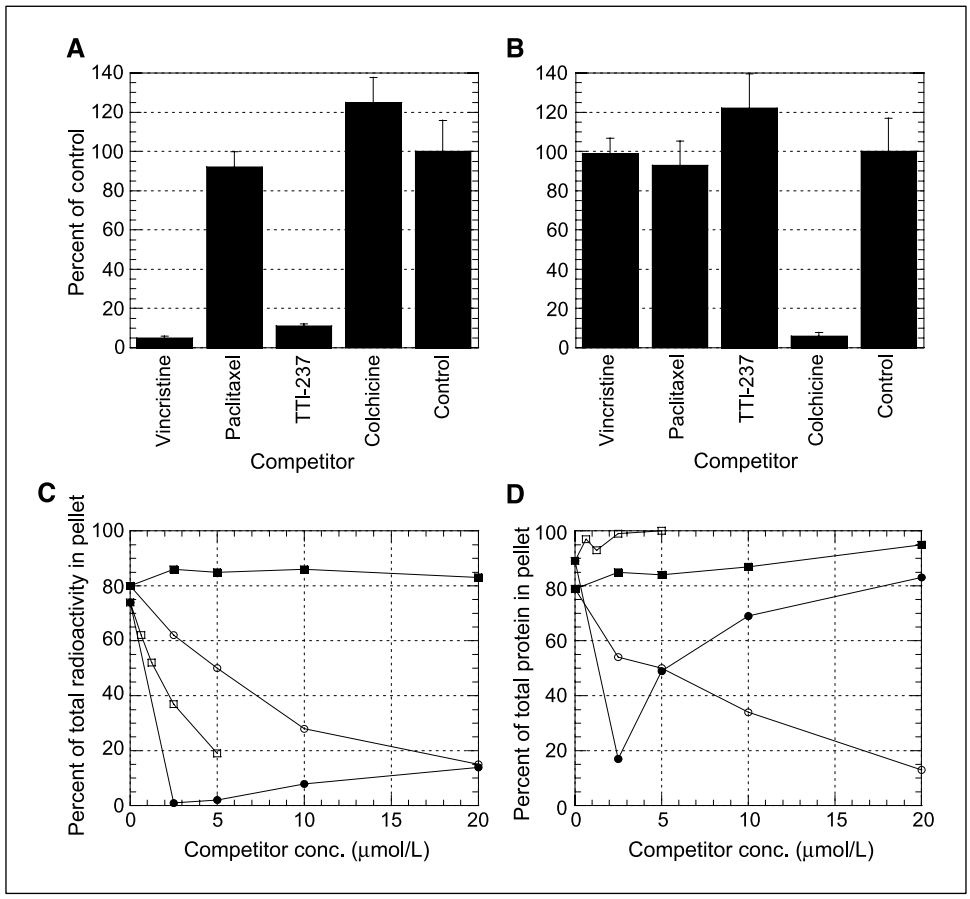

Figure 3. Competitive binding studies. *A,* competition of the indicated compounds at 100 μmol/L with [^{3}H]vinblastine for binding to purified tubulin heterodimer. *B,* competition of the indicated compounds at 100 μmol/L with [^{3}H]colchicine for binding to purified tubulin heterodimer. Both *A* and *B* present pooled data from two independent experiments, eight replicates in total for each; *bars,* SD. DMSO concentrations ranged from 0.5% to 1%; controls received an amount of DMSO equal to the highest experimental samples. *C* and *D,* competition with [^{3}H]paclitaxel for binding to preformed microtubules. *C,* percentage of total radioactivity found in sedimentable microtubules. *D,* percentage of total protein found in sedimentable microtubules. For both graphs: ●, vincristine; □, paclitaxel; ○, colchicine; ■, TTI-237. Data in *C* and *D* are from single experiments; similar results were obtained in at least two additional independent experiments for all compounds. DMSO concentrations ranged from 0.625% to 5%; controls received an amount of DMSO equal to the highest experimental samples.

and above. The lag phase was greatly reduced or eliminated, and the curves assumed a hyperbolic rather than S-shaped appearance (Fig. 2*A*). Concentrations of 8.1 and 24.3 μmol/L TTI-237 (TTI-237 in rough molar equivalence and molar excess over tubulin, respectively) produced hyperbolic curves with much higher plateaus. The polymerization curves induced by the same concentrations of docetaxel were also hyperbolic (Supplemetary Fig. S1*A*). Vincristine at 8.1 and 24.3 μmol/L produced hyperbolic aggregation curves, reflecting the property of this compound to induce formation of nonmicrotubule aggregates at high concentrations (ref. 16; Supplementary Fig. S2*A*). The plateaus reached by vincristine-containing reactions were much lower than those reached in the presence of docetaxel or TTI-237. Colchicine, on the other hand, progressively inhibited polymerization of microtubule protein (Supplementary Fig. S3*A*).

Figures 2*B* and *C* show the effect of TTI-237 on the aggregation of microtubule protein without added GTP and on highly purified tubulin with GTP, respectively. In both cases, TTI-237 at some concentrations caused tubulin aggregation. Docetaxel was more potent in both situations (Supplementary Fig. S1*B* and *C*); vincristine at 2.7, 8.1, and 24.3 μmol/L caused aggregation of microtubule protein without added GTP (Supplementary Fig. S2*B*), but the curves continued to increase after a 1-hour reaction time, unlike those of docetaxel and TTI-237 which reached a plateau. Colchicine inhibited the very weak intrinsic polymerization of microtubule protein without added GTP (Supplementary Fig. S3*B*), and neither vincristine nor colchicine had any effect on highly purified tubulin with GTP (Supplementary Figs. S2*C* and S3*C*).

TTI-237 was also able to induce aggregation of highly purified tubulin in the absence of added GTP (Fig. 2*D*). By itself, such tubulin does not spontaneously polymerize. TTI-237 was active only at concentrations of 8.1 and 23.4 μmol/L, i.e., near or above the concentration of tubulin heterodimers. Docetaxel induced measurable polymerization at concentrations as low as 0.1 μmol/L (Supplementary Fig. S1*D*). Vincristine and colchicine did not induce aggregation at any tested concentration (Supplementary Figs. S2*D* and S3*D*).

TTI-237 inhibits binding of vinblastine to tubulin. TTI-237 competed with [^{3}H]vinblastine, but not with [^{3}H]colchicine, for binding to purified tubulin heterodimers. Vincristine and TTI-237 substantially inhibited the binding of [^{3}H]vinblastine to tubulin heterodimers, but colchicine and paclitaxel did not (Fig. 3*A*). In comparison, using the same set of inhibitor compounds, only colchicine inhibited the binding of [^{3}H]colchicine (Fig. 3*B*). Further experiments were done using a range of TTI-237 concentrations to determine whether the inhibition of [^{3}H]vinblastine binding was competitive. However, these experiments yielded inconclusive results, perhaps because the aggregation state of tubulin in the reactions changed with time in the presence of TTI-237 (not shown).

Competition with [^{3}H]paclitaxel for binding to preformed microtubules was done using a sedimentation assay which allowed both the amount of protein in the pellets and the amount of bound radioactivity to be determined (Fig. 3*C* and *D*). Unlabeled paclitaxel strongly inhibited the amount of [^{3}H]paclitaxel recovered in the sedimented pellets, but increased the amount of protein

in the pellets. In contrast, vincristine initially inhibited both protein and radioactivity in the pellets; but as vincristine concentration increased, the amount of protein in the pellets also increased whereas the radioactivity in those pellets remained low. This was because vincristine initially depolymerized the preformed microtubules, causing a decrease in both protein and radioactivity in the pellets. At higher vincristine concentrations, nonmicrotubule aggregates which contributed to the increased protein in the pellets were formed. However, [^{3}H]paclitaxel did not bind well to these abnormal aggregates. Colchicine caused a coordinate and concentration-dependent decline in both protein and radioactivity in the sedimented pellets. This reflected the action of colchicine to depolymerize the preformed microtubules without inducing abnormal aggregates. The effects of TTI-237 in this assay were different from those of any of these reference compounds. TTI-237 did not reduce either protein or radioactivity in the sedimented microtubules. This indicated that TTI-237 neither competed with [^{3}H]paclitaxel for binding to microtubules nor depolymerized the microtubules. Such a result is consistent with two interpretations: that TTI-237 does not bind to microtubules at all or it binds at a site distinct from the taxane site without causing microtubule depolymerization. In combination with the other results presented here, the latter interpretation is favored.

Taken together, these competitive binding experiments show that TTI-237 does not bind at the colchicine or taxane sites. We have not yet been able to show whether the inhibition of [^{3}H]vinblastine binding is competitive or allosteric. Therefore, TTI-237 binds either to the *Vinca* domain or to a novel site on tubulin that allosterically affects vinblastine binding.

TTI-237 induces multiple spindle poles and multinuclear cells. Control HeLa cells had predominantly single nuclei and well-formed, highly detailed microtubule networks (Fig. 4*A*). Aberrant cells were rare, and mitoses were normal (not shown). At concentrations as low as 17 nmol/L, TTI-237 caused the appearance of extra centrosome-like microtubule organizing centers in some mitotic cells, although the overall frequency of mitotic cells was not increased; these organizing centers were apparently functional, as judged by the Y-shaped structure of chromatin (Supplementary Fig. S4*A*). Figure 4*B* shows a cell that appears to be dividing into triplets, and each of the progeny cells seems to be binuclear or at least to have a bilobed nucleus. At 34 nmol/L (near its IC_{50} value of 40 nmol/L on HeLa cells), TTI-237 continued to induce abnormal, multipolar mitotic spindles (Supplementary Fig. S4*B*). Other images (not shown) revealed that although many of the mitotic figures were abnormal, the mitotic index at this concentration was not changed substantially from control. Thus, TTI-237 did not induce mitotic arrest of HeLa cells at this concentration. Instead, many of the cells with abnormal spindles seemed to continue through mitosis and reenter G_1 phase with multiple nuclei (typically 2–4). Figure 4*C* shows that these multinuclear cells had reformed interphase microtubules that seemed similar to those in control cells (Fig. 4*A*). At 68 nmol/L with HeLa cells, TTI-237 caused a strong mitotic block (Fig. 4*D*). The blocked cells were characterized by having three to eight dense clusters of microtubules. Microtubules in interphase cells still seemed normal (not shown). At no concentration up to 1 μmol/L did TTI-237 induce the bundling of interphase microtubules that is characteristic of taxanes.

By comparison, paclitaxel, at low concentrations (around its cytotoxic IC_{50} value of 3 nmol/L in a 3-day cytotoxicity assay) and at early times (18–20 hours after addition to cells), did not induce a mitotic block, but rather produced mitotic cells with multiple tubulin nucleation centers (refs. 17–21 and data not shown). These cells were able to proceed through mitosis, producing progeny G_1 cells with multiple nuclei as a result of failed or abnormal cytokinesis (18). In contrast, vincristine and colchicine caused a weak mitotic block at 20 hours at concentrations around their IC_{50} values (2 and 20 nmol/L, respectively) and did not produce significant numbers of multinuclear cells (ref. 17 and data not shown).

TTI-237 produces sub-G_1 nuclei at a concentration lower than that required for mitotic block. Detailed evaluations of the effects of TTI-237 on cell cycle progression as a function of concentration were carried out, using a flow cytometry procedure

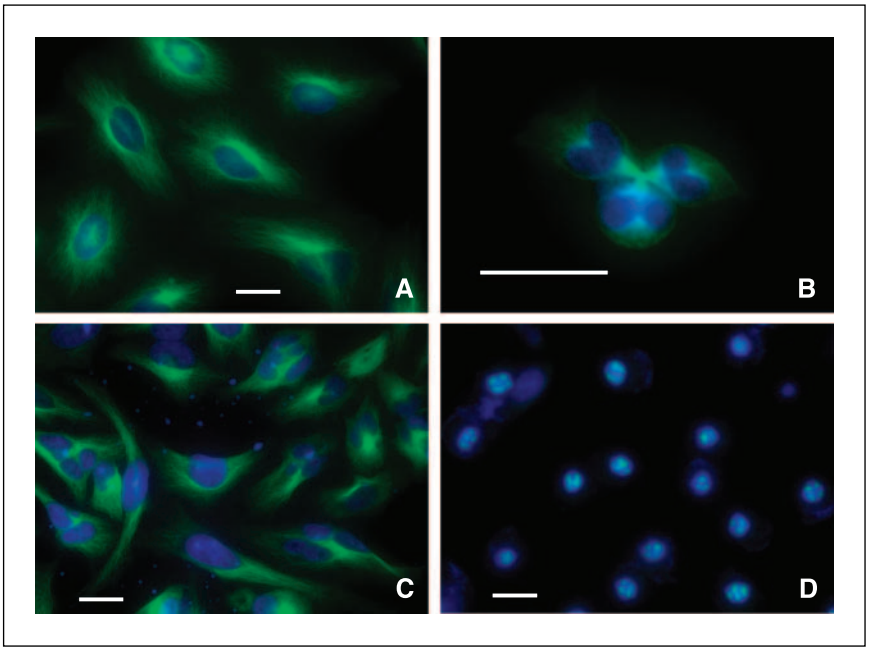

Figure 4. Tubulin immunofluorescence of HeLa cells with TTI-237. HeLa cells were cultured for 20 h with TTI-237 at the following concentrations: *A,* control, no TTI-237; *B,* 17 nmol/L; *C,* 34 nmol/L; *D,* 68 nmol/L. DMSO was present in cultures at a final concentration of 0.007% or lower. Tubulin was stained with a monoclonal anti–α-tubulin antibody and a goat second antibody conjugated to fluorescein (*green*); chromatin was stained with Hoechst 33258 (*blue*). *Bars,* 25 μm.

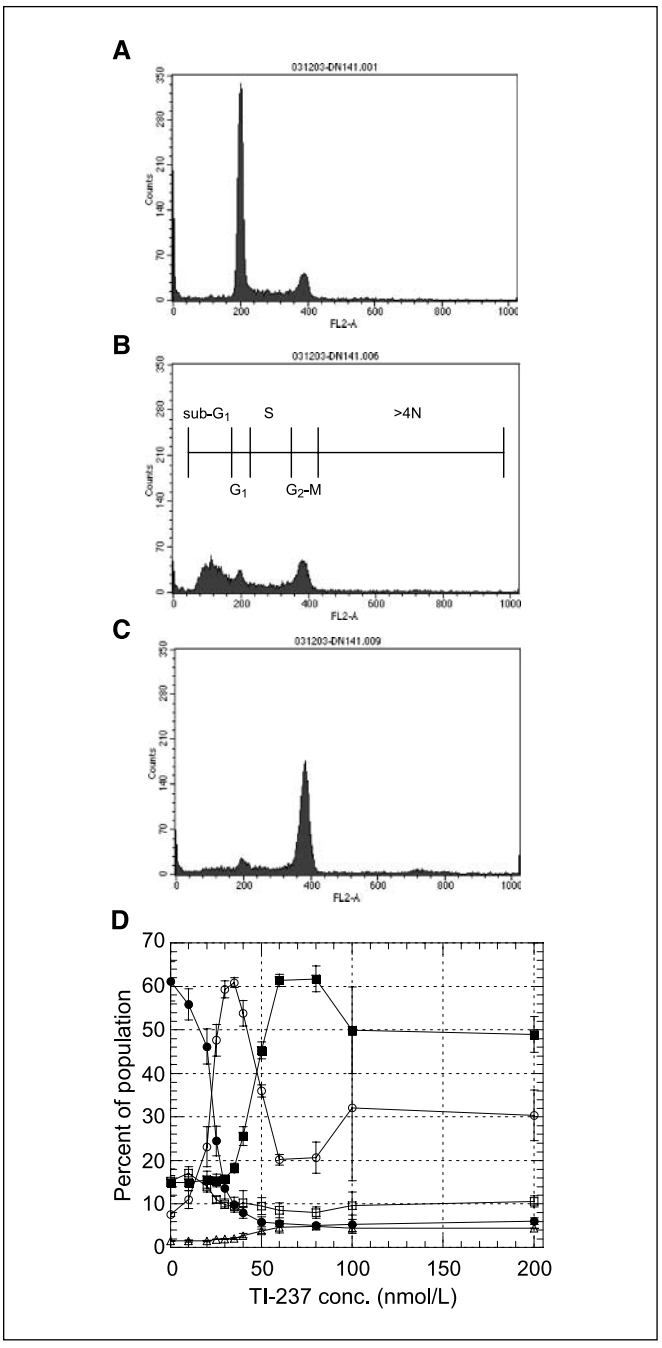

Figure 5. Cell cycle analysis of HeLa cells cultured for 18 h with TTI-237. *A-C,* population histograms from the flow cytometer. *A,* control cells, no compound; *B,* 34 nmol/L TTI-237; *C,* 80 nmol/L TTI-237. *D,* concentration dependence of the cell cycle phases induced by TTI-237. ○, sub-G_1 fraction; ●, G_1 fraction; □, S fraction; ■, G_2-M fraction; △, >4N fraction. Data are pooled from three independent experiments; *bars,* SD. All cultures contained a final concentration of 0.5% DMSO.

that determined the DNA content of washed and stabilized nuclei obtained from treated cells. In the absence of compound, ~61% of the counted nuclei were in G_1 phase, 15% were in S phase, and 15% were in G_2-M phase (Fig. 5*A* and *D*). In addition, ~8% had a sub-G_1 (or <2N) DNA content, and 1% had >4N content. As TTI-237 concentration increased from 10 to 35 nmol/L (20-hour incubation), there was a sharp decline in the G_1 population and a corresponding increase in the sub-G_1 population, which reached ~60% of the total nuclei counted at its peak; there was little change in the S, G_2-M, or >4N populations (Fig. 5*B* and *D*). At concentrations higher than 35 nmol/L, the sub-G_1 peak fell and the G_2-M peak increased (Fig. 5*C* and *D*), reaching plateau values that remained constant to 200 nmol/L.

Docetaxel also produced a strong peak of sub-G_1 nuclei at concentrations around its cytotoxic IC_{50} value (~1 nmol/L), without an increase in the G_2-M population (Supplementary Fig. S5*A*). At higher concentrations, the sub-G_1 population declined and the G_2-M population increased, but these changes were not as dramatic as with TTI-237. Vincristine and colchicine, on the other hand, did not produce peaks of sub-G_1 nuclei at any tested concentration (Supplementary Fig. S5*B* and *C*). Rather, with both compounds, there was a gradual increase in the sub-G_1 population that paralleled the increase in G_2-M.

Cytotoxic activity of TTI-237. Multiple batches of TTI-237, including the free base form, hydrochloride, and succinate salts, were tested in a 3-day cytotoxicity assay with COLO 205 cells over a period of many months. The mean IC_{50} value ± SD from 43 assays was 34 ± 10 nmol/L. There were no differences in activity among the free base and salt forms. IC_{50} values for several reference compounds in this assay are given in Supplementary Table S1.

The cytotoxic activity of TTI-237 was also tested on several other human tumor cell lines from various tissues (Supplementary Table S2). The compound showed good activity (between 18 and 40 nmol/L IC_{50} values) on lines from ovarian, breast, prostate, and cervical tumors.

TTI-237 is a poor substrate of P-glycoprotein. The activity of TTI-237 against cells expressing the MDR1 multidrug resistance transporter, P-glycoprotein, was assessed in two lines derived from human KB epidermoid carcinoma cells. KB, the parental line, expresses no P-glycoprotein; KB-8-5 expresses a moderate level of P-glycoprotein, and KB-VI expresses a very high level. The recognition of a compound by P-glycoprotein can be assessed by the resistance ratio, which is the ratio of the IC_{50} value on the resistant line to that on the sensitive parental line. Results for TTI-237, paclitaxel, vincristine, colchicine, and several other compounds, are shown in Supplementary Table S3. The resistance ratio for TTI-237 on KB-8-5 was 2.9, indicating very little resistance, whereas the values for paclitaxel and vincristine were 11 and 26, respectively. On the highly expressing KB-VI line, the ratios for TTI-237, paclitaxel, and vincristine were 25, 806, and 925, respectively. Therefore, TTI-237 is a poor substrate of the P-glycoprotein transporter and retains substantial activity against lines expressing this protein.

Similar experiments on appropriate nonexpressing and expressing cell lines showed that TTI-237 was not a substrate of the MRP or MXR transporters (Supplementary Tables S4 and S5).

TTI-237 is active by i.v. and p.o. administration against human tumor xenografts. Because of the successful clinical use of *Vinca* alkaloids and taxanes in the treatment of cancer, TTI-237 was tested for antitumor efficacy in two mouse xenograft models. In the first, the compound, which has excellent solubility in water, was formulated in 0.9% saline and given i.v. to athymic mice bearing staged tumors of LoVo human colon adenocarcinoma. The compound was given every 4 days for four cycles at doses of 5, 10, 15, and 20 mg/kg/dose. The compound showed dose-dependent effects, with good antitumor activity at 20 and 15 mg/kg (Fig. 6*A*).

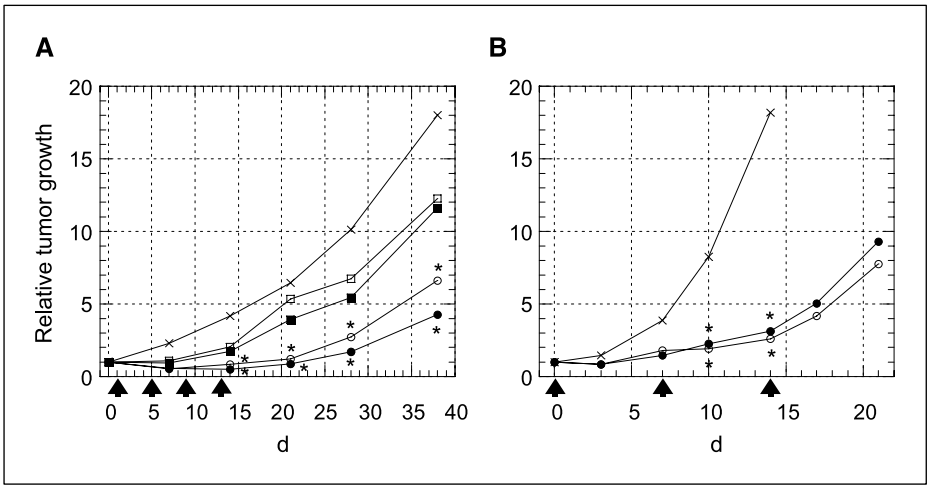

Figure 6. *In vivo* antitumor activity of TTI-237 in mouse xenograft models. *A,* activity against LoVo human colon adenocarcinoma tumors. The compound was given to tumor-bearing mice by i.v. injection on days 1, 5, 9, and 13 (*arrows*) after staging, at the following doses: ×, vehicle control; ●, 20 mg/kg/dose; ○, 15 mg/kg/dose; ■, 10 mg/kg/dose; □, 5 mg/kg/dose. Vehicle was 0.9% saline. Pooled data from two independent experiments: $n = 20$ for control group, $n = 10$ for each experimental group. *B,* activity against U87-MG human glioblastoma. The compound was given to tumor-bearing mice at 25 mg/kg/dose on days 0, 7, and 14 (*arrows*) after staging either by i.v. injection (○) or p.o. gavage (●). The control group (×) received vehicle only (Klucel) by i.v. injection. The control group contained 10 animals and each experimental group contained nine animals. In both panels, the * indicates values significantly different than control.

In the second model, U87-MG human glioblastoma, TTI-237 was given both i.v. and p.o. at a single dose of 25 mg/kg to tumor-bearing mice. The compound was about equally effective by the two routes (Fig. 6*B*).

Discussion

TTI-237 is unusual among tubulin ligands because (*a*) it displaces [^{3}H]vinblastine from the αβ-heterodimer but it does not depolymerize microtubules; it does not displace [^{3}H]colchicine or [^{3}H]paclitaxel; (*b*) it promotes the aggregation of both microtubule protein and purified tubulin in biochemical assays; and (*c*) it promotes the formation of multiple centrosome-like microtubule organizing centers and multinuclear cells, like paclitaxel, but it does not cause microtubule bundling. The compound is also potent, fully synthetic, of fairly simple structure, water soluble, not a good substrate of P-glycoprotein, and shows *in vivo* activity. Thus, there is a reasonable expectation that TTI-237 could show efficacious effects in cancer patients.

Most examples of tubulin-polymerizing small molecules are natural products of complex structure, e.g., taxanes, including paclitaxel and docetaxel, epothilones (22), discodermolide (23), sarcodictyins (24), eleutherobins (25), laulimalides (26), peloruside A (27), dictyostatins (28), cyclostreptin (29), and taccalonolides (30), some of which are not water soluble and/or not available in large quantities. Among this group, only paclitaxel and docetaxel have achieved clinical approval, although several of these classes offer promising future prospects (31).

The compounds that seem to be most similar to TTI-237 in pharmacologic properties are rhazinilam (32) and ceratamines A and B (33). (−)-Rhazinilam, derived from a natural product of complicated structure during isolation, induced the formation of anomalous tubulin assemblies (spirals). This process was prevented by vinblastine and maytansine, but not by colchicine. Saturable and stoichiometric binding of radioactive rhazinilam to tubulin in spirals was reported, and binding was abolished in the presence of vinblastine and maytansine. In contrast, specific binding of radioactive rhazinilam to tubulin assembled in microtubules was undetectable. These findings may be analogous to our results in Fig. 3*C* and *D* that TTI-237 did not affect either the binding of [^{3}H]paclitaxel to or the protein content of preformed microtubules. (−)-Rhazinilam showed no *in vivo* activity, probably due to CYP2B6 oxidation (34). Therefore, the rhazinilam structure must serve as a guide to the synthesis of more active compounds (35).

Ceratamines A and B (33) are another class of natural product that may be similar in action to TTI-237. These sea sponge-derived alkaloids of relatively simple structures are considerably less potent than TTI-237 and have not yet been shown to have *in vivo* antixenograft activity. They caused a concentration-dependent block in cell cycle progression at mitosis, and biochemical studies with purified tubulin indicated that they directly stimulated microtubule polymerization in the absence of MAPs. Cells treated with ceratamines showed a dense perinuclear microtubule network in interphase and multiple pillar-like tubulin structures in mitotic cells. The ceratamines did not compete with paclitaxel for binding to microtubules.

Several other synthetic small molecules have been reported to enhance tubulin polymerization (36–40). GS-164 (36), which is not structurally related to TTI-237, stimulated the assembly of microtubule proteins *in vitro* in a concentration-dependent and GTP-independent manner. GS-164 in the micromolar range arrested the cell cycle of HeLa cells in the mitotic phase leading to cell death, and it increased the amounts of cellular microtubules in HeLa cells, resulting in the formation of microtubule bundles. However, the binding site of GS-164 was not identified, and the cytotoxicity of GS-164 against human tumor cells was several hundred-fold lower than that of paclitaxel, making GS-164 itself a lead for the synthesis of more useful compounds.

The compound reported by Mayer et al. (37) and Haggerty et al. (41), called synstab A, polymerized microtubules from purified tubulin. It produced microtubule bundles in interphase cells, but it had an IC_{50} of ~15 μmol/L in a cytoblot assay. Synstab A displaced a fluorescently labeled paclitaxel analogue from stabilized microtubules, so it presumably was bound in the paclitaxel site.

Trapidil (Rocornal) is a name given to a triazolopyrimidine that has been used clinically for many years (not available in the United States and some European countries). The structure of trapidil is 5-methyl-7-diethylamino-1,2,4-triazolo[1,5-a]pyrimidine, and thus, its side chains and side chain locations are different than TTI-237. Trapidil is reported to have a number of biological activities, but its *in vivo* mechanisms of action are poorly defined. An antitubulin activity has not been described for trapidil.

The aggregates of tubulin induced by TTI-237 have not yet been analyzed electron microscopically to determine whether they are real microtubules or an aberrant polymeric structure. If

TTI-237 is indeed a *Vinca*-site ligand and induces abnormal nonmicrotubule polymers of tubulin as vincristine does, then TTI-237 is unusual in that it does not cause microtubule depolymerization as other *Vinca*-site ligands do, it induces aggregation under conditions in which vincristine does not and it would be the first fully synthetic chemotype of high potency for this site yet described. On the other hand, TTI-237 might bind at a novel site, distinct from the *Vinca*, colchicine, or taxane sites. Interestingly, both laulimalide (42) and peloruside A (43) induce microtubule assembly by binding to sites distinct from the taxane site.

The immunofluorescence images in Fig. 4 suggest that TTI-237 does not grossly disrupt interphase microtubules at compound concentrations where it has a clear effect on mitotic microtubules. This observation may have consequences for possible toxicities in patients. Peripheral neuropathies, important and often dose-limiting side effects of some tubulin-active drugs, are thought to be caused by the disruptive actions of these drugs on interphase microtubules in nerve cells. Peripheral neuropathies may be minimized in patients taking TTI-237 compared with other microtubule-active drugs.

The sub-G_1 nuclei detected by flow cytometry in Fig. 5*D* probably came mainly from the multinuclear interphase cells seen in the immunofluorescence images (Fig. 4*C*). The highest frequency of multinuclear cells and the sub-G_1 peak both occurred over the same range of TTI-237 concentrations ($\sim$25–40 nmol/L). Furthermore, in both cell cycle and immunofluorescence experiments, cells were analyzed 18 to 20 hours after compound addition. This period of time would allow only one cycle of DNA replication for most cells, so the maximum amount of DNA in most cells would be a 4N amount. Multiple nuclei derived from a cell initially having a 4N amount of DNA would, on average, have less than a 2N amount, i.e., a sub-G_1 amount, of DNA. Another source of the sub-G_1 nuclei detected by flow cytometry, especially in the cases of vincristine and colchicine, could be apoptosis. It has been reported that the multinuclear cells produced by low concentrations of paclitaxel undergo apoptosis (18), and apoptotic nuclear fragments are typically found in the sub-G_1 region of cell cycle histograms (44). Further experiments will be required to determine the relative contributions of apoptosis and fragmentation of multinuclear cells to the sub-G_1 population.

The absence of a G_2-M block in cell cycle analysis (Fig. 5*D*) at the concentrations of TTI-237 that caused peak levels of sub-G_1 nuclei (25–40 nmol/L) is consistent with the immunofluorescence observation that there was no increase in the mitotic index at these same concentrations. At higher TTI-237 concentrations (>60 nmol/L), the substantial increase in the G_2-M population agrees with the immunofluorescence observation of cells blocked in mitosis (Fig. 4*D*).

In summary, TTI-237, a novel, potent, synthetic small molecule, inhibits binding of vinblastine at the *Vinca* alkaloid site of the $\alpha\beta$-tubulin heterodimer. It enhances the aggregation of microtubule protein at substoichiometric concentrations and also induces aggregation of highly purified tubulin in the absence of GTP. At low concentrations with cells, TTI-237 induces mitotic spindle perturbations that do not cause mitotic block but lead to the production of multinuclear G_1 cells. TTI-237 shows good antitumor activity in nude mouse xenograft models of human cancer.

Acknowledgments

Received 4/16/2007; revised 11/13/2007; accepted 1/8/2008.

The costs of publication of this article were defrayed in part by the payment of page charges. This article must therefore be hereby marked *advertisement* in accordance with 18 U.S.C. Section 1734 solely to indicate this fact.

References

1. Nogales E. Structural insights into microtubule function. Annu Rev Biochem 2000;69:277–302.
2. Wood KW, Cornwell WD, Jackson JR. Past and future of the mitotic spindle as an oncology target. Curr Opin Pharmacol 2001;1:370–7.
3. Checchi PM, Nettles JH, Zhou J, Snyder JP, Joshi HC. Microtubule-interacting drugs for cancer treatment. Trends Pharmacol Sci 2003;24:361–5.
4. Jordan MA, Wilson L. Microtubules as a target for anticancer drugs. Nat Rev Cancer 2004;4:253–65.
5. Zhou J, Giannakakou P. Targeting microtubules for cancer chemotherapy. Curr Med Chem Anti-Canc Agents 2005;5:65–71.
6. Bhalla KN. Microtubule-targeted anticancer agents and apoptosis. Oncogene 2003;22:9075–86.
7. Pellegrini F, Budman DR. Review: tubulin function, action of antitubulin drugs, and new drug development. Cancer Invest 2005;23:264–73.
8. Jackson JR, Patrick DR, Dar MM, Huang PS. Targeted anti-mitotic therapies: can we improve on tubulin agents? Nat Rev Cancer 2007;7:107–17.
9. Hamel E. Antimitotic natural products and their interactions with tubulin. Med Res Rev 1996;16:207–31.
10. Hamel E, Covell DG. Antimitotic peptides and depsipeptides. Curr Med Chem Anti-Canc Agents 2002; 2:19–53.
11. Stachel SJ, Biswas K, Danishefsky SJ. The epothilones, eleutherobins, and related types of molecules. Curr Pharm Des 2001;7:1277–90.
12. Zhang N, Ayral-Kaloustian S, Nguyen T, et al. Synthesis and SAR of [1,2,4]triazolo[1,5-*a*]pyrimidines, a class of anticancer agents with a unique mechanism of tubulin inhibition. J Med Chem 2007;50:319–27.
13. Shen DW, Cardarelli C, Hwang J, et al. Multiple drug-resistant human KB carcinoma cells independently selected for high-level resistance to colchicine, adriamycin, or vinblastine show changes in expression of specific proteins. J Biol Chem 1986; 261:7762–70.
14. Hamel E, Sackett DL, Vourloumis D, Nicolaou KC. The coral-derived natural products eleutherobin and sarcodictyins A and B: effects on the assembly of purified tubulin with and without microtubule-associated proteins and binding at the polymer taxoid site. Biochemistry 1999;38:5490–8.
15. Darzynkiewicz Z, Juan G, Bedner E. Determining cell cycle stages by flow cytometry. In: Bonifacino JS, Dasso M, Harford JB, Lippincott-Schwartz J, Yamada KM, editors. Current Protocols in Cell Biology. New York: John Wiley & Sons, Inc.; 1999. p. 8.4.1-8.4.18.
16. Lobert S, Vulevic B, Correia JJ. Interaction of *Vinca* alkaloids with tubulin: a comparison of vinblastine, vincristine, and vinorelbine. Biochem 1996;35:6806–14.
17. Chen JG, Horwitz SB. Differential mitotic responses to microtubule-stabilizing and -destabilizing drugs. Cancer Res 2002;62:1935–8.
18. Jordan MA, Wendell K, Gardiner S, Derry WB, Copp H, Wilson L. Mitotic block induced in HeLa cells by low concentrations of paclitaxel (Taxol) results in abnormal mitotic exit and apoptotic cell death. Cancer Res 1996; 56:816–25.
19. Paoletti A, Giocanti N, Favaudon V, Bornens M. Pulse treatment of interphasic HeLa cells with nanomolar doses of docetaxel affects centrosome organization and leads to catastrophic exit of mitosis. J Cell Sci 1997;110: 2403–15.
20. Torres K, Horwitz SB. Mechanisms of taxol-induced cell death are concentration dependent. Cancer Res 1998;58:3620–6.
21. Motwani M, Li XK, Schwartz GK. Flavopiridol, a cyclin-dependent kinase inhibitor, prevents spindle inhibitor-induced endoreduplication in human cancer cells. Clin Cancer Res 2000;6:924–32.
22. Bollag DM, McQueney PA, Zhu J, et al. Epothilones, a new class of microtubule-stabilizing agents with a taxol-like mechanism of action. Cancer Res 1995;55:2325–33.
23. ter Haar E, Kowalski RJ, Hamel E, et al. Discodermolide, a cytotoxic marine agent that stabilizes microtubules more potently than taxol. Biochemistry 1996;35:243–50.
24. Ciomei M, Albanese C, Pastori W, et al. Sarcodictyins: a new class of marine derivatives with mode of action similar to Taxol. Proc Am Assoc Cancer Res 1997;38:5.
25. Long BH, Carboni JM, Wasserman AJ, et al. Eleutherobin, a novel cytotoxic agent that induces tubulin polymerization, is similar to paclitaxel (Taxol). Cancer Res 1998;58:1111–5.
26. Mooberry SL, Tien G, Hernandez AH, Plubrukarn A, Davidson BS. Laulimalide and isolaulimalide, new paclitaxel-like microtubule-stabilizing agents. Cancer Res 1999;59:653–60.
27. Hood DA, West LM, Rouwe B, et al. Peloruside A, a novel antimitotic agent with paclitaxel-like microtubule-stabilizing activity. Cancer Res 2002;62:3356–60.
28. Isbrucker RA, Cummins J, Pomponi SA, Longley RE, Wright AE. Tubulin polymerizing activity of dictyostatin-1, a polyketide of marine sponge origin. Biochem Pharmacol 2003;66:75–82.
29. Edler MC, Buey RM, Gussio R, et al. Cyclostreptin (FR182877), an antitumor tubulin-polymerizing agent deficient in enhancing tubulin assembly despite its high affinity for the taxoid site. Biochemistry 2005;44: 11525–38.

30. Tinley TL, Randall-Hlubek DA, Leal RM, et al. Taccalonolides E and A: plant-derived steroids with microtubule-stabilizing activity. Cancer Res 2003;63: 3211–20.

31. Chou T-C, Dong H, Zhang X, Tong WP, Danishefsky SJ. Therapeutic cure against human tumor xenografts in nude mice by a microtubule stabilization agent, Fludelone, via parenteral or oral route. Cancer Res 2005;65:9445–54.

32. David B, Sevenet T, Morgat M, et al. Rhazinilam mimics the cellular effects of Taxol by different mechanisms of action. Cell Motil Cytoskeleton 1994;28:317–26.

33. Karjala G, Chan Q, Manzo E, Andersen RJ, Roberge M. Ceratamines, structurally simple microtubule-stabilizing antimitotic agents with unusual cellular effects. Cancer Res 2005;65:3040–3.

34. Decor A, Bellocq D, Thoison O, et al. *In vitro* oxidative metabolism study of (-)-rhazinilam. Bioorg Med Chem 2006;14:1558–64.

35. Decor A, Monse B, Martin M-T, et al. Synthesis and biological evaluation of B-ring analogues of (-)-rhazinilam. Bioorg Med Chem 2006;14:2314–32.

36. Shintani Y, Tanaka T, Nozaki Y. GS-164, a small synthetic compound, stimulates tubulin polymerization by a similar mechanism to that of taxol. Cancer Chemother Pharmacol 1997;40:513–20.

37. Mayer TU, Kapoor TM, Haggarty SJ, King RW, Schreiber SL, Mitchison TJ. Small molecule inhibitor of mitotic spindle bipolarity identified in a phenotype-based screen. Science 1999;286:971–4.

38. Li P-K, Pandit B, Sackett DL, et al. A thalidomide analogue with *in vitro* antiproliferative, antimitotic, and microtubule-stabilizing activities. Mol Cancer Ther 2006;5:450–6.

39. Wang Z, Yang D, Mohanakrishnan AK, et al. Synthesis of B-ring homologated estradiol analogues that modulate tubulin polymerization and microtubule stability. J Med Chem 2000;43:2419–29.

40. Markelewicz RJ, Jr., Hall SJ, Beokelheide K. 2,5-Hexanedione and carbendazim coexposure synergistically disrupts rat spermatogenesis despite opposing molecular effects on microtubules. Toxicol Sci 2004;80: 92–100.

41. Haggarty SJ, Mayer TU, Miyamoto DT, et al. Dissecting cellular processes using small molecules: identification of colchicine-like, taxol-like and other small molecules that perturb mitosis. Chem Biol 2000;7:275–86.

42. Pryor DE, O'Brate A, Bilcer G, et al. The microtubule stabilizing agent laulimalide does not bind in the taxoid site, kills cells resistant to paclitaxel and epothilones, and may not require its epoxide moiety for activity. Biochemistry 2002;41:9109–15.

43. Gaitanos TN, Buey RM, Diaz JF, et al. Peloruside A does not bind to the taxoid site on β-tubulin and retains its activity in multidrug-resistant cell lines. Cancer Res 2004;64:5063–7.

44. Darzynkiewicz Z, Juan G, Li X, Gorczyca W, Murakami T, Traganos F. Cytometry in cell necrobiology: analysis of apoptosis and accidental cell death (necrosis). Cytometry 1997;27:1–20.